IEEE Access
Multidisciplinary | Rapid Review | Open Access Journal

Received April 21, 2017, accepted May 11, 2017, date of publication May 23, 2017, date of current version June 28, 2017.

Digital Object Identifier 10.1109/ACCESS.2017.2707384

Novel Approach to Non-Invasive Blood Glucose Monitoring Based on Transmittance and Refraction of Visible Laser Light

HAIDER ALI, FAYCAL BENSAALI, (Senior Member, IEEE), AND FADI JABER, (Member, IEEE)
Department of Electrical Engineering, Qatar University, Doha 2713, Qatar
Corresponding author: Haider Ali (ha1517983@qu.edu.qa)

ABSTRACT Current blood glucose monitoring (BGM) techniques are invasive as they require a finger prick blood sample, a repetitively painful process that creates the risk of infection. BGM is essential to avoid complications arising due to abnormal blood glucose levels in diabetic patients. Laser light-based sensors have demonstrated a superior potential for BGM. Existing near-infrared (NIR)-based BGM techniques have shortcomings, such as the absorption of light in human tissue, higher signal-to-noise ratio, and lower accuracy, and these disadvantages have prevented NIR techniques from being employed for commercial BGM applications. A simple, compact, and cost-effective non-invasive device using visible red laser light of wavelength 650 nm for BGM (RL-BGM) is implemented in this paper. The RL-BGM monitoring device has three major technical advantages over NIR. Unlike NIR, red laser light has ∼30 times better transmittance through human tissue. Furthermore, when compared with NIR, the refractive index of laser light is more sensitive to the variations in glucose level concentration resulting in faster response times ∼7–10 s. Red laser light also demonstrates both higher linearity and accuracy for BGM. The designed RL-BGM device has been tested for both *in vitro* and *in vivo* cases and several experimental results have been generated to ensure the accuracy and precision of the proposed BGM sensor.

INDEX TERMS Absorbance, blood glucose monitoring, in-vitro, in-vivo, laser circular spot (LCS), optical density, refractive index, transmittance.

I. INTRODUCTION

Diabetes or Diabetes Mellitus occurs when someone has abnormal blood sugar [1]. There are two major types of diabetes in Type 1 diabetic patients, diabetes occurs due to the autoimmune destruction of the insulin-producing beta cells in the pancreas whereas in Type 2 diabetics the diabetes mellitus occurs from insulin resistance and relative insulin deficiency [2], [3]. Diabetes can cause many serious secondary health issues such as blindness, stroke, kidney failure, Ulcers, Infections, obesity and blood vessels damage, among other health complications [4]–[6]. Approximately US $ 376 billion is spent annually in the US on the treatment and management of diabetes in diabetic patients and this amount is expected to rise to a projected US$ 490 billion by the end of 2030 [7], [11]. According to the International Diabetes Federation (IDF) the diabetes patients in 2011 are 366 million worldwide and this number is expected to rise to 552 million by 2030 [8], [9]. Blood glucose concentration is currently measured using three broad categories of techniques which are invasive, minimally invasive and non-invasive. Invasive techniques require a blood sample which is currently extracted from the fingertip using a device known as a lancet. This method of determining blood glucose is currently the most commonly used technique and is a highly accurate method for blood glucose monitoring [10]. Minimally invasive techniques involve attaching electrodes to the skin tissue. This method is not preferred due to its low accuracy and poor signal to noise ratio (SNR) even though this electronic method reduces the chances of infection and minimizes the pain [11]. The latest advances introduced to the field of BGM are non-invasive technologies to detect blood glucose concentration using secretions such as sweat, urine, saliva or tears. Besides these secreted fluids glucose concentration is also measured through the skin, earlobe and tongue tissue [11]–[17]. These mediums are analyzed to detect glucose concentration non-invasively by employing optical techniques such as Raman spectroscopy, polarimetry, diffuse reflection spectroscopy, absorption spectroscopy,

thermal emission spectroscopy, photoacoustic spectroscopy and fluorescence spectroscopy [12], [18], [19]. Among the available non-invasive techniques absorption spectroscopy is mostly used to observe scattering, absorption, reflection and refraction of light when it is focused on biological tissues. The characteristics of light depend on the chemical composition and structure of the sample [10], [20].

Researchers and scientists for the development of new BGM technologies have more focused on the area of near-infrared spectroscopy (NIRS) rather than on other areas of non-invasive glucose level detection [18]. Mohd Zain *et al.* [21] introduced a technique to generate an attenuated polarized 785 nm wavelength beam from diode laser and directed it towards the glucose sample. When the beam is passed through the sample, the weak coherent laser light is coupled to a fiber and then connected to a photon counting system. This research demonstrated that the photon counts per second and glucose concentration have a linear correlation in samples with glucose concentrations from 10 mg.dL^{-1} to 260 mg.dL^{-1}. Another research performed by Abidin *et al.* [22] developed a system by using NIR of wavelengths 940 nm and 950 nm generated from an LED to observe the transmittance of light. The measured output voltage from photo-sensor increased with increasing glucose concentrations. In this experiment, in-vivo results are generated using human finger and observed the output voltage variations before and after a meal for both the aforementioned wavelengths. Anas *et al.* [23] designed a device using NIR transmitter and placed it on the human fingertip to detect the variations in light. The output voltage from photodiode indicated the blood glucose concentration for fasting and non-fasting. Paul *et al.* [24] in their research showed that as the glucose concentration increases, a reduction in the scattering coefficient occurred and the light intensity increased at the sensor. Buda and Addi [25] proposed a portable device with an accuracy of 84% using near infrared light to display glucose concentration and the required dose of insulin was designed and presented in their paper. Similarly, several other researchers have explored the area of NIR for non-invasive BGM using the transmittance characteristics of laser light [15]–[17].

Existing experimental non-invasive sensors are based on near-infrared (NIR), the main drawbacks of these NIR sensors include cost, light absorption in biological chromospheres, stratum corneum that alters the accuracy as well SNR and the sensors dependency on the ambient environment. These disadvantages of NIR based BGM have prevented medical and commercial applications for this seemingly advantageous and non-invasive technique [12]–[14]. Regular blood glucose monitoring plays a significant role in diabetes management and health care as there is no cure for diabetes [13]. Currently, BGM which in some cases must be performed several times a day relies on a crude technique that involves puncturing the skin to draw a drop of blood. Additionally, the technique relies on the use of blood test machines with expensive test strips as consumables raising concerns of running costs thereby decreasing the frequency of testing by patients as well as the issue of the skin puncture in addition to the generated medical waste [12], [14]. The development of a non-invasive and accurate BGM device will be a sigh of relief for diabetic patients who are forced to employ this invasive technique.

In this paper, the suitable wavelength of laser light for BGM is investigated by determining the transmittance and absorbance of various wavelengths when passed through water and the human finger. On the basis of this suitable wavelength, a simple, non-invasive, cost effective blood glucose level detection technique and device (RL-BGM) based on the variations in the refractive index of red laser light is presented. Intensification of glucose concentration increases the refractive index which consequently steps up the output voltage at the photo-sensor. The variations in output voltage are converted into equivalent glucose concentrations level. Hardware for both in-vitro and in-vivo cases have been fabricated and tested.

II. PROPOSED WORK

A. WORKING PRINCIPLE

Glucose molecules have the ability to vary the refractive angle of light to an extent proportional to its concentration, and the overall refractive index of a given media [26]–[29]. Refraction based estimation is based on the principle of Snell's law and the magnitude of each parameter is related to the concentration of glucose in the aqueous solution. According to Snell's law, the refractive angle is inversely proportional to the concentration of glucose in aqueous sample. The light ray (*ab)* in Fig. 1 tends to incline towards the normal *ac* and decreases the refractive angle ($\theta 2$) as the glucose concentration increases hence more photons strike the photo-transistor.

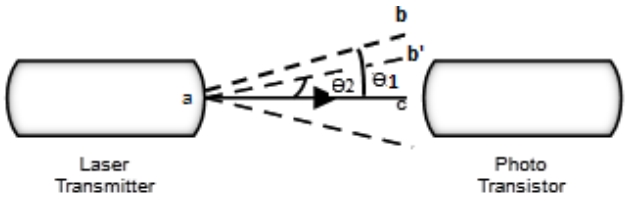

FIGURE 1. Refractive angle decreases with the increase in glucose-D concentration in GCSs.

The relation between output voltage (Voc') and light intensity (X) is expressed in (1). Simplification of equation (1) results in a direct relation between the intensity of light and output voltage as shown in (2). Each photon carries $3.056e^{-37}$J of energy as expressed in (3), higher number of photons striking the photo-transistor's surface in return generates the higher output voltage (Voc'). The refractive index ($n2$) for various glucose concentration is measured by joining points a, b and c of Fig. 1. The glucose concentration rise in aqueous solution reduces the refractive angle ($\theta 2$) and the line ab reaches to a new position ab'. Refractive index ($n2$) is calculated using a mathematical form of the

Snell's law using (4). The refractive angle ($\theta 2$) decreases for higher glucose concentrations which consequently increases the refractive index ($n2$) according to (4) and the output voltage (Voc') rises as more number of photons strike the phototransistor. Reduction in $\theta 2$ also decreases the radius (bc) of the laser circular spot (LCS) as light rays bend towards the normal (ac) shown in Fig. 1 at higher glucose concentrations according to Snell's law.

$$Voc' = \frac{nkT}{q} \ln\left(\frac{XIsc}{Io}\right) = \frac{nkT}{q}\left[\ln\left(\frac{Isc}{Io}\right) + \ln X\right]$$
$$Voc' = (Voc) + \frac{nkT}{q} \ln X \tag{1}$$

Where,

I_O = Reverse saturation current

I_{SC} = Short circuit current

Voc = Initial voltage

$\frac{nkT}{q}$ = Constant at a temperature (T) while, q=1.602×10^{-19} and k = 1.380×10^{-23}. All the parameters except intensity of light (X) are constant. Therefore,

$$Voc' \propto \ln X \tag{2}$$

The amount of energy that each photon carries is

$$E = \frac{hC}{\lambda} \tag{3}$$

While the variables in (3) have the values, $h = 6.6260 \times 10^{-34}$m^2 kg / s, $C = 2.9 \times 10^8$ m /s and $\lambda = 650$ nm.

Equation (3) shows that the energy possessed by the photon is dependent on the wavelength hence photons of NIR light (700-1400 nm) carry lesser energy than red light (650 nm). This mathematical analysis potentially suggests that red light is suitable for biomedical applications as the absorbance of red light will be lesser than NIR due to its higher energy.

Snell's law is represented mathematically by equation (4a).

$$n2 = \frac{n1\,(\sin\theta 1)}{\sin\theta 2} \tag{4a}$$

Where, $n1 = 1.333$ representing the refractive index of water, $n2$ is the refractive index of aqueous glucose solution which is to be determined, $\theta 1$ represents the refractive angle of water and $\theta 2$ shows the refractive angle of the glucose solution. The refractive angles $\theta 1$, $\theta 2$ are calculated by using the following equations (4b), and (4c) which are derived from the triangles Δ abc and Δab'c respectively in Fig. 1.

$$\theta 1 = \tan^{-1}\left(\frac{bc}{ac}\right) \tag{4b}$$

$$\theta 2 = \tan^{-1}\left(\frac{b'c}{ac}\right) \tag{4c}$$

While bc represents the radius of the LCS for water and $b'c$ is the radius for the glucose concentration solution (GCS) of the LCS image, whereas ac is a fixed distance of 279.4 mm. The parameter $\theta 2$ for GCS is a variable that changes with glucose-D concentration.

The refractive index ($n2$) is calculated only for the GCS (in-vitro) as the output LCS for the human finger has no clear boundaries. In case of the human finger the effect of light refraction due to the variations in blood glucose level is observed in terms of the changes in the output voltage.

B. OPTIMUM WAVELENGTH SELECTION

The optimum wavelength for BGM was determined by passing visible and NIR light starting from 500 nm wavelength to 1200 nm wavelengths through water using a spectrophotometer. The obtained experimental results are expressed in transmittance (T), which shows the ratio of the radiant powers for water sample shown mathematically in (5). The absorbance of each wavelength through the water can be calculated by using (6). This experiment was also repeated for the human finger in order to determine the transmittance and optical density (OD). As the Human finger is a complex medium where the striking laser light can possibly reflect, refract, absorb, scatter and transmit depending upon the nature of the light [30], [31]. Wavelengths of laser light from 500 nm to 1200 nm are generated using LEDS of 1.5 watt power (Po) and the generated laser light is passed through the human finger. The transmitted light through the human finger is measured using (5) as a ratio between the output power (P) at the phototransistor and the power (Po) when laser light directly falls on the phototransistor, when there is no human finger inserted in the RL-BGM. The transmittance is converted into OD by using (7) and the absorbance can be estimated by employing (8). OD measures the throughput of the human finger whereas OD is directly related to the transmittance [32].

$$Transmittance\,(T) = \frac{P}{Po} \tag{5}$$

Where, P is the radiant power of the rays leaving water or human finger and P_o is the radiant power for monochromatic laser light.

$$Absorbance\,(A) = -\log\left(\frac{\%T}{100}\right) \tag{6}$$

The transmittance of human finger was measured using (7).

$$T = 10^{-OD} \tag{7}$$

Where, OD = Optical density of the human finger.

$$A = 2 - \log(\%T) \tag{8}$$

C. IN-VITRO EXPERIMENTAL SETUP

Glucose concentrations samples are prepared by dissolving glucose-D in distilled water and aqueous solutions in concentrations of {50, 100, 150, 200, 250, 300, 350, 400, 450} mg.dL^{-1} are prepared at room temperature (22 C°). A container (cuvette) made of 2.81mm thick glass having width 15.77 mm, length 50.87 mm and height 150 mm (volume = 1.2×10^5mm) holds the glucose concentration samples (GCSs) for the experiment. Fig. 2 illustrates RL-BGM for in-vitro case. The RL-BGM consists of laser light transmitter that

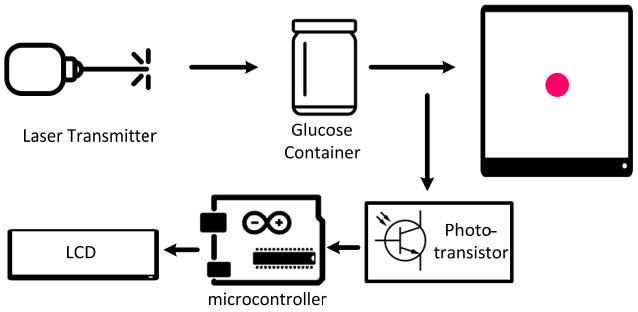

FIGURE 2. RL-BGM device for in-vitro measurement of the output voltage and refractive index of various GCSs.

generates laser light of wavelength 650 nm, directed towards the container and LCS is observed on the screen. The radius of LCS is measured using digital caliper for various GCSs and the refractive index $n2$ values are calculated by using (4a). Once the refractive indexes for GCSs are calculated then the photo-transistor is placed between the container and the screen such that the transmitted light from the cuvette falls on the phototransistor and the output voltages (Voc') are measured at Photo-transistor for various GCSs using the fabricated RL-BGM device. Photo-transistor measures the intensity of light in voltage (mV) and Arduino-Uno microcontroller displays the output results on LCD display. The output voltage at the photo-transistor is checked with both voltmeter and displayed on LCD to ensure that both the readings are the same.

D. IN-VITRO LCS IMAGE PROCESSING

Human error may occur while measuring the radii of the LCSs, therefore an alternative method is also applied using an image processing technique.

DSLR 600D, (136 mm) is kept at a fixed distance and angle in a dark room to take the pictures of LCS for various GCSs. The photographs are converted into gray scale and the radii in pixels are calculated for GCSs in order to determine the correlation of the number of pixels with glucose-D concentrations in GCSs. The steps followed for calculating the radii of GCSs are illustrated in Fig. 3.

E. IN-VIVO EXPERIMENTAL SETUP

Whole rat blood is used in the glucose container to observe the output voltage (Vo) response at the photo-sensor with the time to determine the settling time. The experiment on the human finger is also performed through the designed RL-BGM hardware where, the human finger is inserted into the finger hose of the RL-BGM revealed in Fig. 4 and laser light is passed through it. The variations in blood glucose levels are observed on the voltmeter and the results are also displayed on LCD using the microcontroller. The main purpose of measuring the output voltage through voltmeter and LCD is to make sure that there is no difference between the two voltages as an error in the output voltage can affect the actual reading of the glucose level.

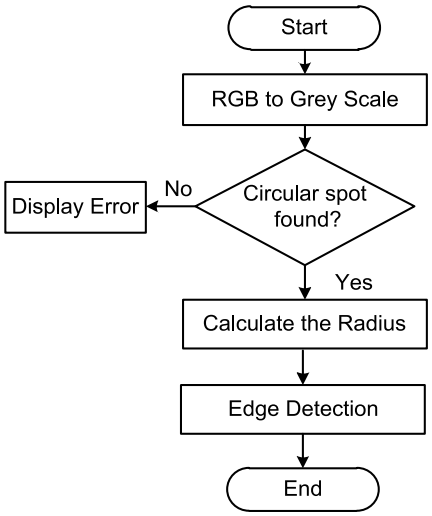

FIGURE 3. Steps for LCS images radii calculations based on counting the number of pixels for each GCS.

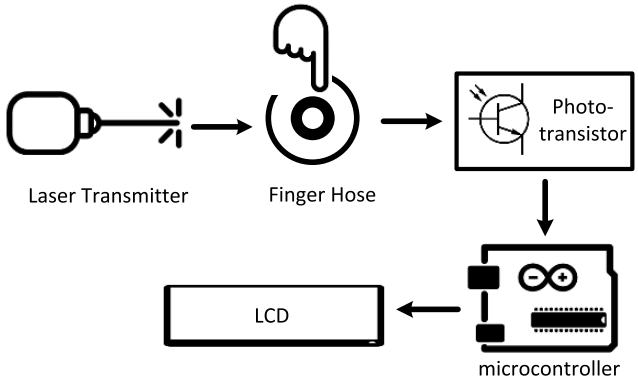

FIGURE 4. In-vivo non-invasive RL-BGM device.

III. HARDWARE IMPLEMENTATION

Compact hardware is designed and fabricated for the proposed technique and tested for both in-vitro and in-vivo cases. The schematics and operations of the hardware are explained in below sections.

A. IN-VITRO HARDWARE IMPLEMENTATION

The main components of the proposed in-vitro system are laser transmitter and photo-sensor. The transmitter connected with +5V DC generates 650 nm uninterruptable laser light using KY-008. The photo-sensor has wavelength sensitivity of 600 nm to 800 nm and detects the laser light passed through glucose sample to convert the optical energy into electrical energy.

The output voltage detected by the photo-sensor depends on the intensity of the received laser light. The photo-sensor is actually a photo-transistor, connected with two LM358 ICs. The ICs are used as a buffer to prevent attenuation. Resistor-capacitor (RC) cut-off filter is connected before and after the

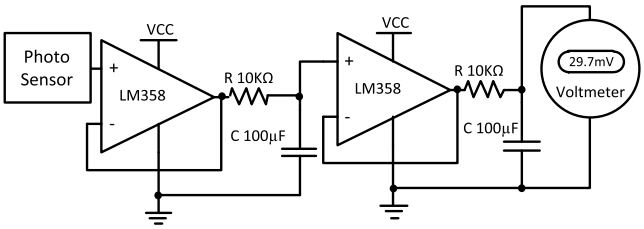

FIGURE 5. Photo-sensor laser light variations detector of non-invasive RL-BGM device.

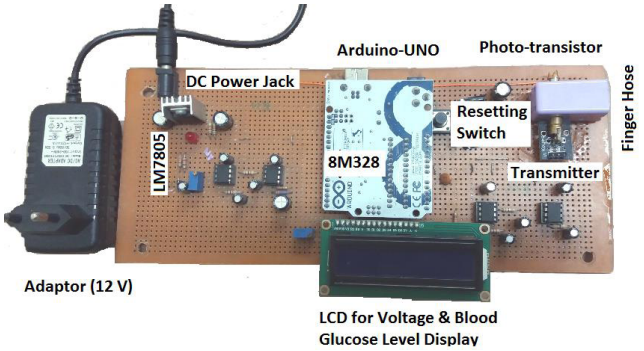

FIGURE 6. Photograph of the fabricated RL-BGM device.

buffer to provide actual DC input to the voltmeter and LCD. The schematic diagram for photo-sensor (receiver) is shown in Fig. 5.

RC filter cut off frequency is calculated using (9).

$$fo = \frac{1}{2\pi RC} \tag{9}$$

Where, R=10 KΩ and C=100 μF

These values are selected such that the overall impedance is much higher than the driving stage output impedance. Using (9) we calculated the cutoff frequency which is 0.15∼0 Hz, so frequencies from the source and surrounding that may alter output voltage are grounded (blocked) through the capacitor and the actual DC output voltage from the photo-sensor is observed on the voltmeter and LCD.

B. IN-VIVO HARDWARE IMPLEMENTATION

In-vivo glucose level detection system is exhibited and labeled in Fig. 6. The hardware consists of 650 nm wavelength transmitter, a photo-sensor to measure light intensity in voltage (mV), RC filter with cut-off frequency 0.15∼0 Hz to remove the noise from the actual signal. Other elements of the RL-BGM are Arduino-UNO microcontroller (8M328), connected with PC and LM061 LCD (2×16) to display the output voltage. The finger hose holds the human finger as well blocking the ambient light. The average cross-sectional area of female's index finger is 1.9-2.6 cm^2 and male's average cross-sectional area is between 2.6 to3.6 cm^2 [2]. The finger hose dimensions are set such that it has 1.8 cm width, 2.2 cm length, and 3 cm depth. A DC power jack with LM7805 IC in the RL-BGM device is deployed to supply power to the system by connecting it with an adaptor of output voltage ranging from +5 V to +12 V. LM7805 IC acts as a voltage regulator and provides a constant +5 V DC voltage. The output voltage in mV from the photo-sensor is displayed on LCD for 5 seconds and then for the next 5 seconds the LCD displays the blood glucose level in mg.dL^{-1}.

IV. IMPLEMENTATION RESULTS AND DISCUSSIONS

The suitable wavelength for BGM is determined experimentally by measuring the transmittance and absorbance of different wavelengths of light ranging from 500 nm to 1200 nm in steps of 50 nm. The light is passed through water and the human finger. The results concluded that the absorption of laser light differs with the wavelength. The highest absorbance is of NIR of wavelengths from 700 nm to 1000 nm making it the least suitable for BGM applications. Red laser light of 650 nm has the capability of penetrating into the water and the human finger as it has the highest % transmittance as compared to other wavelengths.

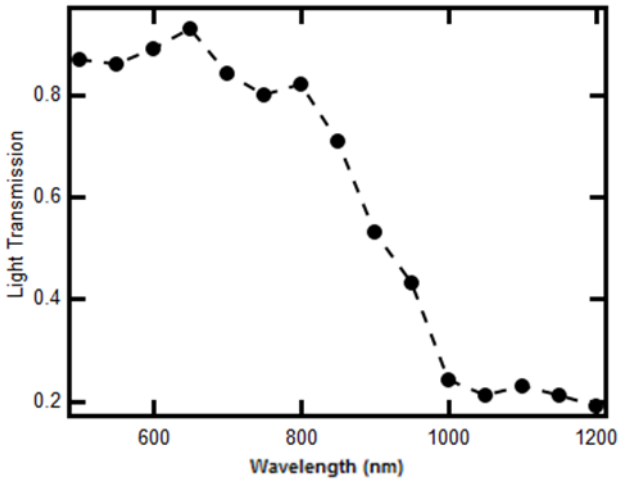

FIGURE 7. The transmittance of visible and NIR laser light through water.

Fig. 7 shows light transmittance for various wavelengths. Red laser light has the highest transmittance of 95% & the lowest absorbance of 0.022 calculated by using (6) making it the most suitable wavelength for light based BGM applications. The phenomenon of transmittance potentially recommends 650 nm as an ideal choice for BGM as water constitutes from 50% to 75% of the human blood composition [12]. The transmittance of light NIR decreases as wavelength increases.

Fig. 8 demonstrates that the transmittance of 650 nm wavelength of visible laser light remains significantly constant for glucose-D concentration from 0 mg.dL^{-1} to 450 mg.dL^{-1}. The phenomenon of refraction occurs only for a specific concentration range of glucose-D in GCSs while the transmission of light remains unchanged. On the contrary, the transmittance of NIR further decreases when the glucose concentration of GCS is increased.

The OD values for each wavelength are calculated by using (5) to determine transmittance (T) first and then

TABLE 1. Average values of different parameters for in-vitro glucose level measurement using RL-BGM device at 22 C°.

Glucose Concentration ($mg.dL^{-1}$)	Glucose Concentration ($mm.L^{-1}$)	Diameters (mm)	Radius (mm)	Refractive angle θ_2 (degrees)	Refractive Index (n_2)	No. of Pixels	Output Voltage (mV)
0	0.0	4.65	2.325	0.47677	1.33300	385	560
50	2.8	4.63	2.315	0.47472	1.33876	370	564
100	5.5	4.59	2.295	0.47062	1.35042	335	565
150	8.3	4.56	2.280	0.46753	1.35931	340	570
200	11.1	4.52	2.260	0.46344	1.37134	325	578
250	13.9	4.49	2.245	0.46037	1.38050	315	590
300	16.7	4.45	2.225	0.45627	1.39291	300	600
350	19.6	4.43	2.215	0.45421	1.39919	290	605
400	22.2	4.41	2.205	0.45217	1.40554	270	609
450	25.0	4.40	2.200	0.45114	1.40873	260	612

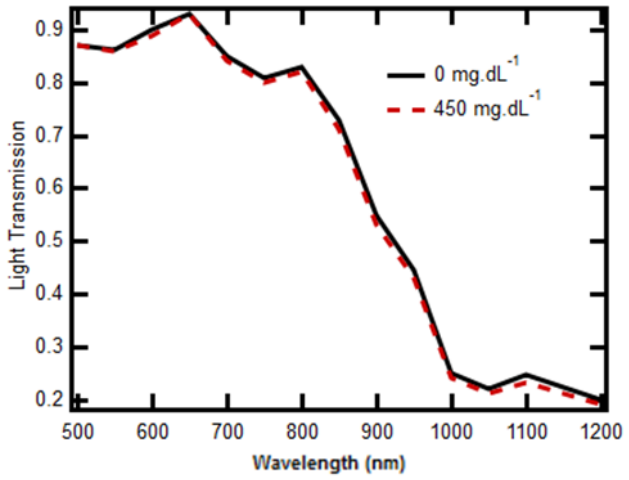

FIGURE 8. The transmittance of red laser light and NIR for glucose-D concentration of 0 $mg.dL^{-1}$ and 450 $mg.dL^{-1}$.

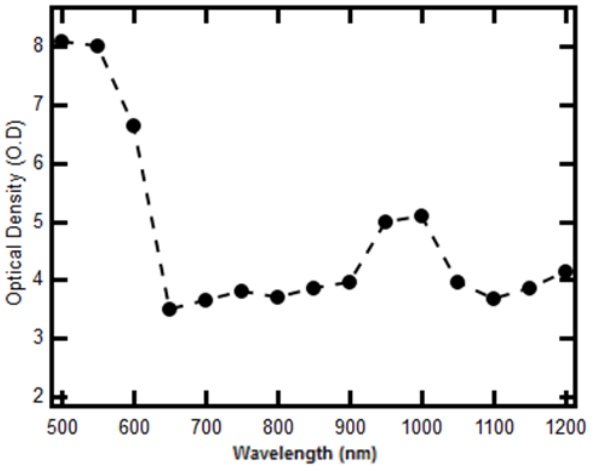

FIGURE 9. The optical (OD) density for 500 nm −1200 nm wavelengths of light when passed through the human finger.

converted into OD by using (7). For instance, when 650 nm light is passed through the human finger it yields an output voltage of 70 mV and current 7 mA at the photo-transistor connected with 10 Ω resistor. The total calculated power (P = IV) at the output resistor is 490 mW. The output power without the human finger is 1.5 W, so by using (5), the transmittance value becomes 0.0326 %. We inserted this transmittance value in (7) which produced 3.5 OD. Similarly, OD values for other wavelengths are also estimated using the same procedure. Each wavelength of light has its own characteristic OD value which describes the transmittance capability of that particular wavelength. Higher the OD value, lower the transmittance and higher the absorbance. Red laser of wavelength 650 nm has the lowest OD value 3.5 when various light wavelengths were passed through a human finger as illustrated in Fig. 9. The figure also illustrates that the OD value for NIR increases when the wavelength is increased. By using (7) we can see that visible light of wavelength 650 nm has the highest transmittance value of 3.2×10^{-4} and NIR of wavelength 950 nm has a transmittance of 1×10^{-5}. The transmittance ratio of both wavelengths suggests that the transmittance of 650 nm wavelength is 30 times higher than NIR 950 nm wavelength. Similarly, by using (8), it gives us the absorbance of red laser light as 3.5 while NIR of wavelength 950 nm demonstrates a much higher absorbance of 5.0. The higher transmittance of wavelength 650 nm laser light makes it a suitable choice of wavelength for BGM.

The refractive index (n_2) for various GCSs is estimated using equation (4a). Table I indicates the average values of different parameters when laser light of 650 nm wavelength is passed through various GCSs 10 times each sample. The experiments are repeated 10 times for each glucose concentrations from 0 $mg.dL^{-1}$ to 450 $mg.dL^{-1}$ in steps of 50 $mg.dL^{-1}$ in order to ensure the repeatability and accuracy of the measured results using RL-BGM device. Experiments were performed in a dark room at a constant temperature of 22 C° in order to minimize the possible effect of these secondary parameters on the original readings.

Dissolving glucose-D in distilled water makes the aqueous solution more viscous and the refractive angle of the incident laser light decreases. Fig. 10 shows that this reduction of angle of refraction concurrently increases the refractive

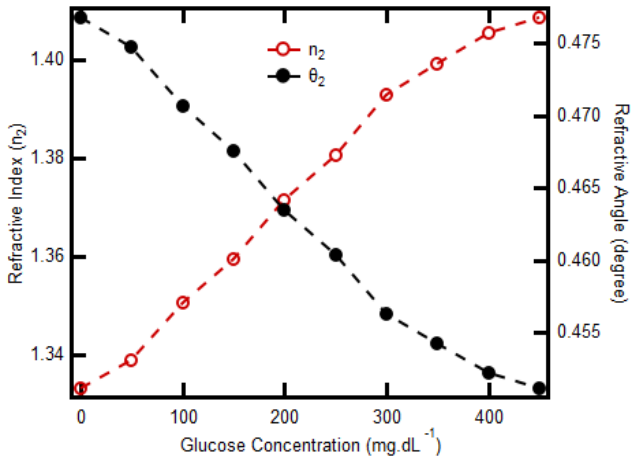

FIGURE 10. Refractive index and refractive angle change when glucose-D concentration is changed in GCS.

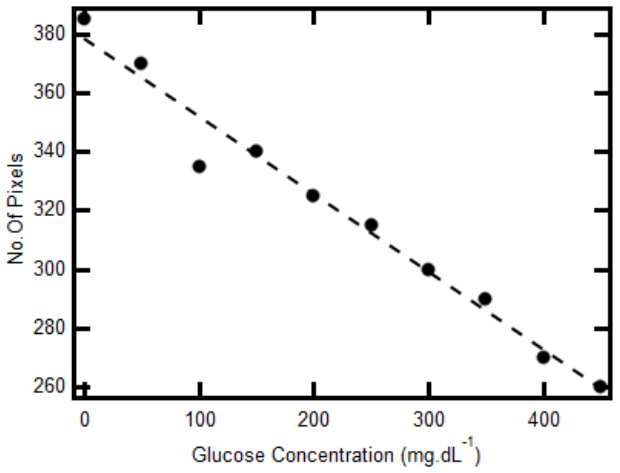

FIGURE 12. The number of pixels in LCS image reduces with the increase in glucose-D concentration in GCSs.

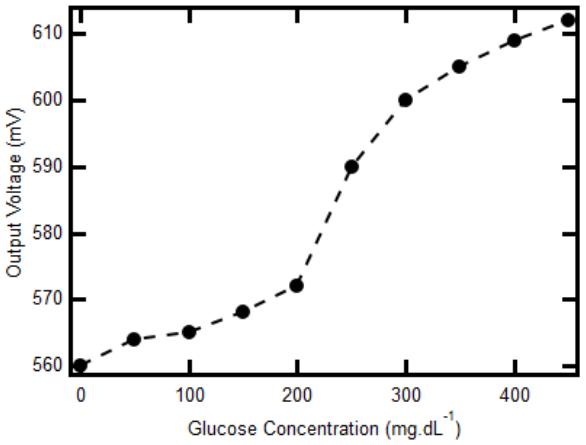

FIGURE 11. Output voltage increases with the glucose-D concentration in GCSs.

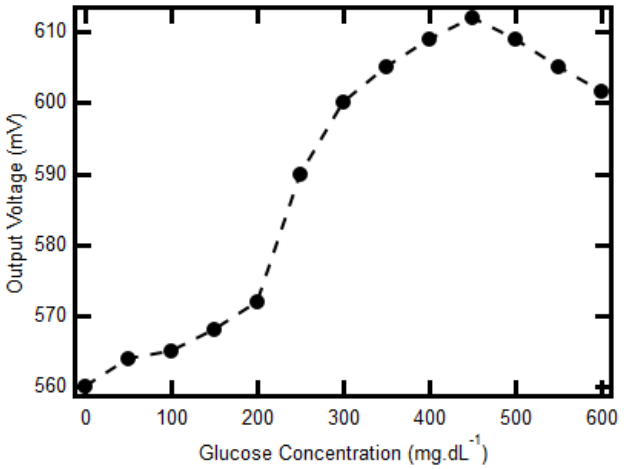

FIGURE 13. Output voltage at the photo-sensor of RL-BGM device for 0 mg.dL^{-1} to 600 mg.dL^{-1} glucose-D concentrations in GCSs.

index of GCSs. The figure also illustrates that the angle of refraction and the refractive index have 98% linearity with the glucose-D concentration in GCSs.

Fig. 11 shows that the output voltage at the photo-sensor starts climbing when glucose-D concentration is increased in the GCSs. The voltage level depends on the amount of glucose-D dissolved in the distilled water. The output voltage (mV) after 130 mg.dL^{-1} has increased sharply and the system exemplifies more sensitivity towards a higher glucose-D level, which makes the designed in- vitro system appropriate in BGM applications for use by diabetic patients. Diabetic patients have blood glucose level >130 mg.dL^{-1} before a meal and it increases after a meal [33]–[35].

The output voltage values were measured 10 times for each GCS. The maximum deviation in the output voltages of ±1 mV was observed and RL-BGM showed ∼ 99 % precision.

Increasing the glucose-D concentration in GCSs reduces the refractive angle of the laser light and consequently reduced the radius of the LCS. This reduction in radius of the LCS shrinks the number of pixels in LCS images as illustrated in Fig. 12. The number of pixels in LCS image and glucose concentration in GCS shows a linearity of 98%.

Fig. 13 shows the output voltage linearity with the concentration of glucose-D in GCSs. The linearity of the curve deviates from the ideal response at a threshold value of 450 mg.dL^{-1} as revealed in the figure. Therefore the fabricated RL-BGM device has a measurement range of 0 mg.dL^{-1} to 450 mg.dL^{-1} equivalent to 0-25 mmole.L^{-1}. The non-linear behavior after 450 mg.dL^{-1} is dependent on the intensity level of the transmitted laser light. Increasing the intensity of laser light results better response at higher concentrations but it lowers the sensitivity for glucose levels below 450 mg.dL^{-1}. This non-linearity shown by the RL-BGM device above the threshold value of 450 mg.dL^{-1} concentration is due to the energy absorption of the glucose molecules [14]. According to Beer's Law, the number

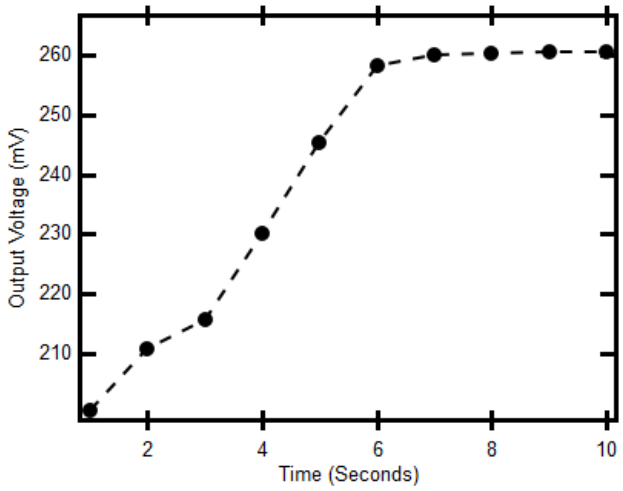

FIGURE 14. Output voltage response of RL-BGM device for whole rat blood.

of collisions of photons with glucose molecules increases significantly such that energy from the photons is absorbed by the glucose molecules at higher concentration [2].

Fig. 14 demonstrates the output voltage at the photo-sensor of the RL-BGM device when laser light is passed through the whole rat blood sample. The output voltage rises and reaches its maximum value after ~ 7 seconds of time. This time spam represents the settling time for RL-BGM device for the whole rat blood sample. This settling time is the response time of RL-BGM device required to measure the blood glucose level.

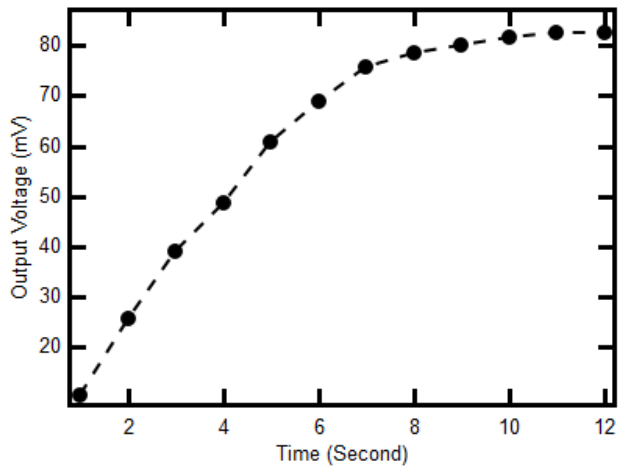

FIGURE 15. Measured in-vivo output voltage of RL-BGM device tested on a healthy subject after meal at 22 C°.

The in-vivo hardware of RL-BGM is tested on a healthy subject to determine the settling time for the RL-BGM device as demonstrated in Fig. 15. Initially, the measured output voltage rises sharply and after 10 seconds the output voltage settles to a maximum voltage value and no further increase occurs. This time spam explicitly describes the response and settling time of the RL-BGM device required BGM.

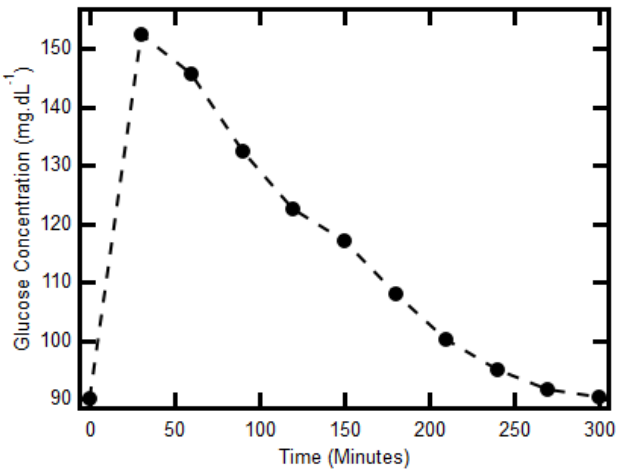

FIGURE 16. Transitions in blood glucose levels of a healthy subject before and after meal measured using RL-BGM device.

Fig. 16 shows the blood glucose concentration before and after a meal for the time duration of 5 hours, tested at intervals of 30 minutes. The voltage 1mV at the photo-sensor of RL-BGM device represents 1.5 mg.dL^{-1} blood glucose concentrations. The RL-BGM device measures the variations in light intensity in terms of voltage and converts this into glucose concentration expressed in mg.dL^{-1}. The Blood glucose concentration of a healthy subject rises rapidly after the meal and drops to the normal blood glucose level after 4 to 5 hours as exhibited in the figure. The rise in blood glucose level is due to the digestion of food and the supply of carbohydrates into the blood [36], [37].

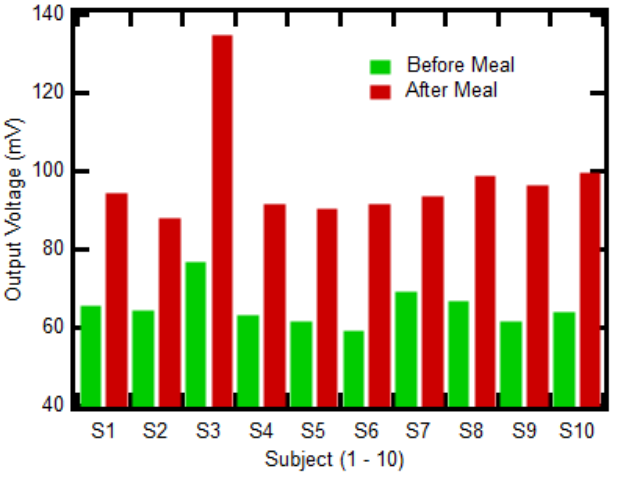

FIGURE 17. RL-BGM device tested on ten subjects for measuring the blood glucose level in voltage form before and after meal.

The precision of the RL-BGM device is further investigated by testing the device on 10 subjects before and after a meal and the output voltages are measured and recorded. Fig. 17 represents the experimental results of the RL-BGM device. Moreover, in the meal a soft drink was also served as it

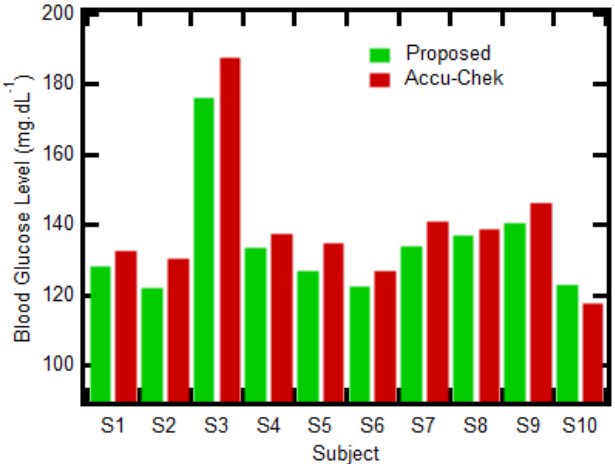

FIGURE 18. RL-BGM device accuracy comparison with the invasive finger prick BGM device Accu-chek.

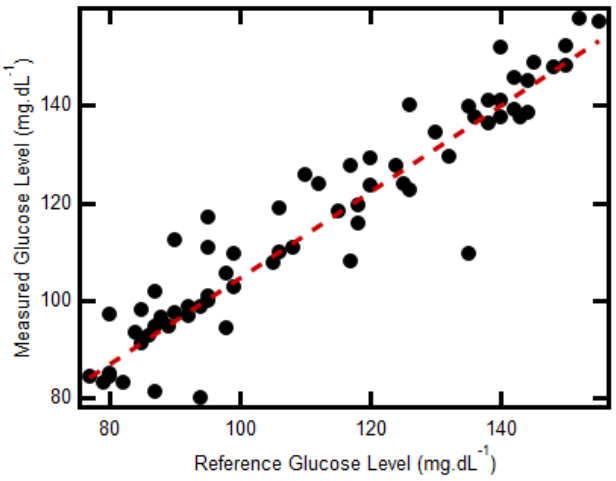

FIGURE 19. Clark Error Grid (CEG) analysis performed for RL-BGM device in order to measure the accuracy.

has a high amount of carbohydrates and soft drinks provide an instant increase in the human blood glucose concentrations. The measured output voltages increased for all 10 subjects after the meal. Subject 3 represented by S3 in Fig. 17, has the highest output voltage before and after meal amongst the 10 subjects tested for blood glucose level in this experiment. These high voltages indicate that subject S3 is pre-diabetic. Other subjects excluding S3 demonstrated a normal increase in the output voltages after this meal.

The accuracy of the RL-GBM device is also verified by comparing the measured blood glucose levels with Accu-chek a standard finger prick BGM device. Fig. 18 shows the reliability test for the RL-BGM device and it illustrates that the measured blood glucose levels using fabricated RL-BGM device are close to the readings from the Accu-chek invasive device. The RL-BGM device deviates 3% - 8% as calculated by using (10). The reasons for deviations are due to variations in human fingers such as the considerable difference in thickness of the finger, cleanliness of the finger and the microscopic swelling of the tissues when absorbing the light energy [14] which is still harmless at such low (3 watt) intensities. These variations can affect the intensity of the output laser light at the photo-transistor and this absorption of light in the tissue disturbs the measured blood glucose level resulting in the 3%-8% deviation of the fabricated RL-BGM device from the Accu-chek results.

$$E_{\%} = \frac{(Glucose)_{Accu-Chek} - (Glucose)_{RL-BGM}}{(Glucose)_{Accu-Chek}}(100) \quad (10)$$

The accuracy and repeatability of RL-BGM is further verified by performing Clark Error Grid (CEG) analysis. The CEG analysis is a reliable procedure for assessing the accuracy and reliability of a medical device. In this method, the measured blood glucose levels are plotted against the reference blood glucose levels [38]. The measured glucose levels of 45 subjects including males and females of age between 20 to 70 years using RL-BGM device are plotted compared to the reference blood glucose levels using Accu-chek as expressed in Fig. 19. Out of the 45 total subjects, 10 of them were tested twice on the same day before and after lunch while the rest of 35 subjects were tested for blood glucose level at least one time either in the morning or afternoon.

Experimental results in Fig. 19 demonstrate that more than 90% of the measured glucose levels using RL-BGM lie in an acceptable range while ∼8%-10% deviate from the reference blood glucose values ∼90%-92% measured experimental values match the reference values). The RL-BGM device exhibits higher accuracy for diabetic patients with blood glucose level >130 mg.dL^{-1} and 96% measured glucose levels match with the reference blood glucose levels (The % average error for glucose level > 130 mg.dL^{-1} is ∼4.). This concludes that RL-BGM device performs more efficiently for blood glucose levels >130 mg.dL^{-1}. The measured results are in the acceptable range following the International Organization for Standardization (ISO) standards [7], [39].

The measured blood glucose level using RL-BGM device can change with temperature as the voltage of the photo-sensor depends on the temperature [40]. RL-BGM illustrates high efficiency at the temperature range 20 C° to 30 C°. Fig. 20 demonstrates that the measured blood glucose levels show an average 0.2% increase with a temperature rise of 1 C°. The device deviation can be significant in harsh environments where the temperature is either very low or very high as compared to room temperature 22 C°. For example, if the temperature is either −10 C° (well below freezing) or 50 C° (torrid heat) then the device may have a deviation of up to 6%.

The fabricated RL-BGM device is independent of the ambient light interference as shown in Fig. 21. The measured blood glucose levels in the dark room and experimental results obtained in the surrounding with ambient light are overlaying each other. This autonomous behavior of the RL-BGM device is due to the finger hose which blocks the light coming into the receiver side from the surrounding.

TABLE 2. Various non-invasive blood glucose monitoring techniques comparison.

Reference	Light Spectrum	Wavelength (nm)	Characteristic Method	Range (mg.dL^{-1})	Linearity (%)	Cost	In-vivo Results
Haxa et al. (2016) [2]	NIR	940	Absorption	>2000<4000	96	High	Yes
Li et al. (2015) [16]	NIR	1310	Transmission	0 – 800	<93	Medium	No
Tamilselvi et al. (2015) [15]	NIR	940	Transmission	120-150	<90	Medium	No
Zain et al. (2014) [21]	NIR	785	Transmission	10 - 260	90	High	No
Buda et al. (2014) [25]	NIR	1450	Absorption	0 - 350	92	Medium	No
Abidin et al. (2013) [22]	NIR	940-950	Transmission	0 – 200	96	Medium	Yes
Abdalsalam et al. (2013) [17]	NIR	700-1400	Scattering	80 - 115	<92	High	No
Anas et al. (2012) [23]	NIR	940	Absorption	72 - 196	15	Medium	Yes
Paul et al. (2012) [24]	NIR-MIR	700-2500	Scattering	130 - 140	90	Medium	Yes
RL-BGM Device	Visible	650	Refraction & Transmission	0 - 450	98	Low	Yes

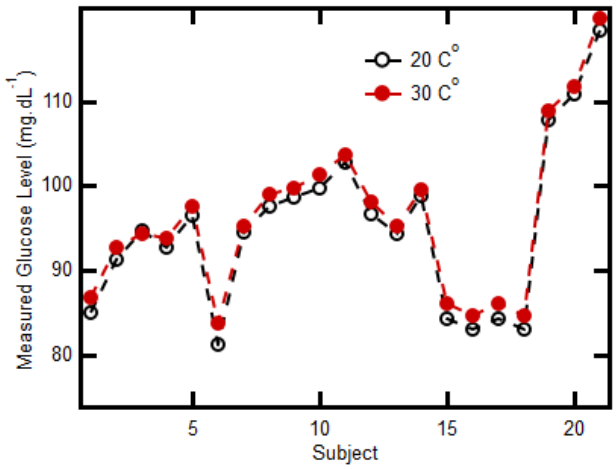

FIGURE 20. Measured human blood glucose levels at different temperatures using RL-BGM device.

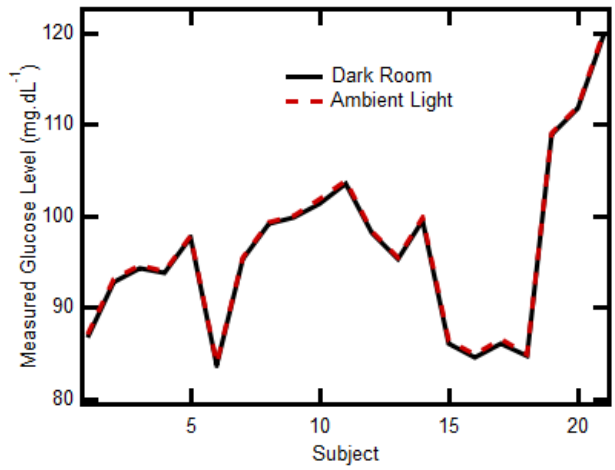

FIGURE 21. RL-BGM device independency on ambient light.

The device accuracy can be affected if exposed to intense light such as direct sunlight.

All the experimental results are generated on the assumption that only blood glucose level variations occur in human blood and parameters like blood pressure and blood cholesterol level are within normal range. The RL-BGM device is tested on normal blood cholesterol level ranging from 200 to 240 mg. dL^{-1} and blood pressure (120/80 mmHg). Blood pressure and cholesterol level of human blood can alter the refractive index, transmittance, and refraction of laser light which may consequently change the output voltage of the device [41]. To test if the RL-BGM device is affected by high cholesterol or high blood pressure we would need to test it on several high blood pressure, high cholesterol and diabetic subjects which would require the permission or approval of the patients and relevant authorities as well as raising ethical questions.

The designed RL-BGM device has been compared with other NIR based BGM techniques because both the methods are non-invasive. The device is compared in terms of parameters like linearity, accuracy, cost, size and in-vitro and in-vivo experimental results as listed in the Table II. RL-BGM device has the highest linearity for in-vitro case as compared to other NIR based BGM sensors [2], [15]–[17], [21]–[25]. RL-BGM device exhibits 98% accuracy in in-vitro case due to utilization of red laser light of 650 nm wavelength. This wavelength has higher transmission and shows higher sensitivity to the glucose level variations as compared to NIR. RL-BGM device is tested for Clark Error Grid (CEG) analysis and tested for in-vivo results. Other NIR based techniques [15]–[17], [21], [25], have merely relied on in-vitro results which are not sufficient to draw conclusions as human tissue and blood are complex mediums [12]. A BGM device's blood glucose measurement range is a critical parameter and most of the NIR based techniques [15], [17], [21]–[25] have a smaller linear range (up to 200 mg.dL^{-1}) for BGM as compared to the fabricated RL-BGM device (up to 450mg.dL^{-1}). BGM device designed in [2] tested at glucose concentration >2000 and <4000 mg.dL^{-1}, which makes it unsuitable for human blood glucose level monitoring. The cost of each NIR based BGM technique is calculated on the basis of components employed, as NIR based sensors have high SNR so higher number of electronic components are required

TABLE 3. Performance summary of the non-invasive RL-BGM device.

Parameters	Value
Linearity	98%
Accuracy	90-92%
Precision	99%
Range	0 $mg.dL^{-1}$ - 450 $mg.dL^{-1}$
Sensitivity	0.66 mV/ $mg.dL^{-1}$
Temperature	20 C^o-30 C^o
Settling Time	7-10 seconds
Limitation	Normal blood pressure & cholesterol level
Laser light Wavelength	650 nm

to process the output light and acquire a minimal acceptable accuracy for BGM [12]. Therefore, NIR based BGM techniques/devices [2], [16], [17], [21]–[25] have the higher number of components as compared to RL-BGM device, that has been fabricated with only four major electronic components. Comparison study also illustrates that none of the NIR based BGM techniques [15]–[17], [21]–[25] has performed CEG analysis in order to determine the accuracy and repeatability of the technique /device.

The key challenges that the next generation continuous BGM devices are facing such as operational cost, sensitivity, and accuracy, precision and settling time for the glucose level measurement [7] are addressed in the fabricated RL-BGM device. RL-BGM has proven superiority over NIR based sensors and techniques as the fabricated device has demonstrated higher linearity and accuracy for both in-vitro and in-vivo cases. The RL-BGM device has also exhibited additional practical advantages such as lower response time ∼7-10 seconds, higher range up to 450 $mg.dL^{-1}$ and higher sensitivity towards glucose level for diabetics with an overall accuracy of 90-92 %.

Table III shows the performance summary, of the RL-BGM device based on the transmittance and refraction phenomena of 650 nm visible laser light.

V. CONCLUSION

This paper presented a potential blood glucose monitoring RL-BGM device. The handheld RL-BGM device operates on +5V and accurately displays blood glucose concentrations within 10 seconds. The RL-BGM device has 4-four main components which are the 650 nm red laser transmitter, photo-sensor, Arduino-UNO and LCD display, the total cost of the components was ∼15$.

Experimental results indicated that red visible light of 650 nm is suitable wavelength for non-invasive BGM. Visible laser light of 650 nm wavelength has 30 times higher transmittance through both water and the human finger as compared to NIR laser light. In-vitro experimental results proved that increasing glucose concentrations in the aqueous solution decreases the refractive angle of the laser light rays and in turn maximizes the intensity of the laser light falling on the photo-sensor which consequently increases the output voltage accordingly. In in-vitro tests, the device showed a linearity of 98% thereby proving its accuracy. The in-vivo testing was performed on 45 subjects both males and females with ages ranging from 20 to 70 years old. This group included both healthy and diabetic patients. The results of the RL-BGM handheld device were checked for accuracy using Clarke Error Grid (CEG) analysis which gave us an overall accuracy of 90%-92% for the RL-BGM device. The reference glucose levels for CEG analysis were obtained with Accu-chek finger prick BGM device.

REFERENCES

[1] S. R. Balakrishnan *et al.*, "Development of highly sensitive polysilicon nanogap with APTES/GOx based lab-on-chip biosensor to determine low levels of salivary glucose," *Sens. Actuators A, Phys.*, vol. 220, pp. 101–111, Dec. 2014.

[2] S. Haxha and J. Jhoja, "Optical based noninvasive glucose monitoring sensor prototype," *IEEE Photon. J.*, vol. 8, no. 6, Dec. 2016, Art. no. 6805911.

[3] W. Duckworth *et al.*, "Glucose control and vascular complications in veterans with type 2 diabetes," *New England J. Med.*, vol. 360, no. 2, pp. 129–139, Jan. 2009.

[4] J. L. Leasher *et al.*, "Global estimates on the number of people blind or visually impaired by diabetic retinopathy: A meta-analysis from 1990 to 2010," *Diabetes Care*, vol. 39, no. 9, pp. 1643–1649, 2016.

[5] "Diagnosis and classification of diabetes mellitus," *Diabetes Care*, vol. 33, no. 1, pp. S62–S69, Dec. 2009.

[6] J. W. Gardner, H. W. Shin, and E. L. Hines, "An electronic nose system to diagnose illness," *Sens. Actuators B, Chem.*, vol. 70, nos. 1–3, pp. 19–24, Nov. 2000.

[7] S. Vashist, "Continuous glucose monitoring systems: A review," *Diagnostics*, vol. 3, no. 4, pp. 385–412, 2013.

[8] D. R. Whiting, L. Guariguata, C. Weil, and J. Shaw, "IDF diabetes atlas: Global estimates of the prevalence of diabetes for 2011 and 2030," *Diabetes Res. Clin. Pract.*, vol. 94, no. 3, pp. 311–321, Dec. 2011.

[9] A. Esteghamati *et al.*, "Trends in the prevalence of diabetes and impaired fasting glucose in association with obesity in Iran: 2005–2011," *Diabetes Res. Clin. Pract.*, vol. 103, no. 2, pp. 319–327, Feb. 2014.

[10] C. E. F. do Amaral and B. Wolf, "Current development in non-invasive glucose monitoring," *Med. Eng. Phys.*, vol. 30, no. 5, pp. 541–549, Jun. 2008.

[11] S. K. Vashist, "Non-invasive glucose monitoring technology in diabetes management: A review," *Anal. Chim. Acta*, vol. 750, pp. 16–27, Oct. 2012.

[12] S. K. Vashist, D. Zheng, K. Al-Rubeaan, J. H. T. Luong, and F.-S. Sheu, "Technology behind commercial devices for blood glucose monitoring in diabetes management: A review," *Anal. Chim. Acta*, vol. 703, no. 2, pp. 124–136, Oct. 2011.

[13] D. Zheng, S. K. Vashist, K. Al-Rubeaan, J. H. T. Luong, and F.-S. Sheu, "Rapid and simple preparation of a reagentless glucose electrochemical biosensor," *Analyst*, vol. 137, no. 16, p. 3800, 2012.

[14] J. Yadav, A. Rani, V. Singh, and B. M. Murari, "Prospects and limitations of non-invasive blood glucose monitoring using near-infrared spectroscopy," *Biomed. Signal Process. Control*, vol. 18, pp. 214–227, Apr. 2015.

[15] M. Tamilselvi and G. Ramkumar, "Non-invasive tracking and monitoring glucose content using near infrared spectroscopy," in *Proc. IEEE Int. Conf. Comput. Intell. Comput. Res. (ICCIC)*, Madurai, India, Dec. 2015, pp. 1–3.

[16] X. Li and C. Li, "Research on non-invasive glucose concentration measurement by NIR transmission," in *Proc. IEEE Int. Conf. Comput. Commun. (ICCC)*, Chengdu, China, Oct. 2015, pp. 223–228.

[17] O. S. Abdalsalam, A.-K. M. Osman, R. M. Abd-Alhadi, and S. D. Alshmaa, "Design of simple noninvasive glucose measuring device," in *Proc. Int. Conf. Comput., Elect. Electron. Eng. (ICCEEE)*, 2013, pp. 216–219.

[18] A. Tura, A. Maran, and G. Pacini, "Non-invasive glucose monitoring: Assessment of technologies and devices according to quantitative criteria," *Diabetes Res. Clin. Pract.*, vol. 77, no. 1, pp. 16–40, Jul. 2007.

[19] A. J. Bandodkar and J. Wang, "Non-invasive wearable electrochemical sensors: A review," *Trends Biotechnol.*, vol. 32, no. 7, pp. 363–371, Jul. 2014.

[20] M. Goodarzi, S. Sharma, H. Ramon, and W. Saeys, "Multivariate calibration of NIR spectroscopic sensors for continuous glucose monitoring," *TrAC Trends Anal. Chem.*, vol. 67, pp. 147–158, Apr. 2015.

[21] M. N. M. Zain, A. Musa, M. H. Hisham, A. R. Laili, and Z. M. Yusof, "Photon counting polarimetry measurement towards non-invasive biomedical glucose monitoring," in *Proc. IEEE 5th Int. Conf. Photon. (ICP)*, Kuala Lumpur, Malaysia, Sep. 2014, pp. 156–158.
[22] M. T. B. Z. Abidin, M. K. R. Rosli, S. A. Shamsuddin, N. K. Madzhi, and M. F. Abdullah, "Initial quantitative comparison of 940 nm and 950 nm infrared sensor performance for measuring glucose non-invasively," in *Proc. IEEE Int. Conf. Smart Instrum., Meas. Appl. (ICSIMA)*, Kuala Lumpur, Malaysia, Nov. 2013, pp. 1–6.
[23] M. N. Anas, N. K. Nurun, A. N. Norali, and M. Normahira, "Non-invasive blood glucose measurement," in *Proc. IEEE-EMBS Conf. Biomed. Eng. Sci.*, Langkawi, Malaysia, Dec. 2012, pp. 503–507.
[24] B. Paul, M. P. Manuel, and Z. C. Alex, "Design and development of non invasive glucose measurement system," in *Proc. 1st Int. Symp. Phys. Technol. Sensors (ISPTS)*, Pune, India, 2012, pp. 43–46.
[25] R. A. Buda and M. M. Addi, "A portable non-invasive blood glucose monitoring device," in *Proc. IEEE Conf. Biomed. Eng. Sci. (IECBES)*, Kuala Lumpur, Malaysia, Dec. 2014, pp. 964–969.
[26] X. Jiang *et al.*, "Immunosensors for detection of pesticide residues," *Biosensors Bioelectron.*, vol. 23, no. 11, pp. 1577–1587, Jun. 2008.
[27] J. S. Maier, S. A. Walker, S. Fantini, M. A. Franceschini, and E. Gratton, "Possible correlation between blood glucose concentration and the reduced scattering coefficient of tissues in the near infrared," *Opt. Lett.*, vol. 19, no. 24, p. 2062, Dec. 1994.
[28] W. Lukosz, "Integrated optical chemical and direct biochemical sensors," *Sens. Actuators B, Chem.*, vol. 29, nos. 1–3, pp. 37–50, Oct. 1995.
[29] D. M. Nathan *et al.*, "Medical management of hyperglycaemia in type 2 diabetes mellitus: A consensus algorithm for the initiation and adjustment of therapy," *Diabetologia*, vol. 52, no. 1, pp. 17–30, Oct. 2008.
[30] C. E. Tedford, S. DeLapp, S. Jacques, and J. Anders, "Quantitative analysis of transcranial and intraparenchymal light penetration in human cadaver brain tissue," *Lasers Surgery Med.*, vol. 47, no. 4, pp. 312–322, Mar. 2015.
[31] W. Wang and C. Li, "Measurement of the light absorption and scattering properties of onion skin and flesh at 633 nm," *Postharvest Biol. Technol.*, vol. 86, pp. 494–501, Dec. 2013.
[32] S. Tassan and G. M. Ferrari, "A sensitivity analysis of the 'transmittanceâĂŞreflectance' method for measuring light absorption by aquatic particles," *J. Plankton Res.*, vol. 24, no. 8, pp. 757–774, Aug. 2002.
[33] F. Cameron, G. Niemeyer, and B. W. Bequette, "Extended multiple model prediction with application to blood glucose regulation," *J. Process Control*, vol. 22, no. 8, pp. 1422–1432, Sep. 2012.
[34] C.-J. Huang, Y.-H. Chen, C.-H. Wang, T.-C. Chou, and G.-B. Lee, "Integrated microfluidic systems for automatic glucose sensing and insulin injection," *Sens. Actuators B, Chem.*, vol. 122, no. 2, pp. 461–468, Mar. 2007.
[35] P. K. Crane *et al.*, "Glucose levels and risk of dementia," *New England J. Med.*, vol. 369, no. 6, pp. 540–548, Aug. 2013.
[36] W. Li *et al.*, "Extraction, degree of polymerization determination and prebiotic effect evaluation of inulin from *Jerusalem artichoke*," *Carbohydrate Polym.*, vol. 121, pp. 315–319, May 2015.
[37] T. L. Setji, B. D. Hong, and M. N. Feinglos, "Technosphere insulin: Inhaled prandial insulin," *Expert Opinion Biol. Therapy*, vol. 16, no. 1, pp. 111–117, Dec. 2015.
[38] B. P. Kovatchev, L. A. Gonder-Frederick, D. J. Cox, and W. L. Clarke, "Evaluating the accuracy of continuous glucose-monitoring sensors: Continuous glucose-error grid analysis illustrated by TheraSense freestyle navigator data," *Diabetes Care*, vol. 27, no. 8, pp. 1922–1928, Jul. 2004.
[39] D. C. Klonoff, "Continuous glucose monitoring: Roadmap for 21st century diabetes therapy," *Diabetes Care*, vol. 28, no. 5, pp. 1231–1239, 2005.
[40] B. Y. Zhang *et al.*, "Broadband high photoresponse from pure monolayer graphene photodetector," *Nature Commun.*, vol. 4, p. 1811, May 2013.
[41] Y. L. Jin, J. Y. Chen, L. Xu, and P. N. Wang, "Refractive index measurement for biomaterial samples by total internal reflection," *Phys. Med. Biol.*, vol. 51, no. 20, pp. N371–N379, Oct. 2006.

HAIDER ALI received the master's degree in electronic systems design engineering from Manchester Metropolitan University, U.K. He is currently pursuing the Ph.D. degree with the Department of Electrical Engineering, Qatar University. He was a Lecturer COMSATS IIT from 2011 to 2016. His research area of interest is electronic and biomedical systems design, image processing and embedded systems.

FAYCAL BENSAALI (S'03–M'06–SM'15) received the Dipl-Ing (M.Eng.) degree in electronics from the University of Constantine and the Ph.D. degree in electronic and computer engineering from Queen's University, Belfast. He is currently an Associate Professor in electrical engineering with Qatar University. He took other academic positions at the University of Hertfordshire-UK and Queen's University Belfast-UK. His research interests are mainly in design and implementation of digital image and signal processing algorithms, custom computing using FPGAs, hardware/software co-design, and system on chip. He is also an HEA Associate.

FADI JABER received the B.Eng. degree in electronic engineering with medical electronics from the University of Kent at Canterbury, U.K., in 2000, the M.Sc. degree in medical physics from the University of Surrey, U.K., in 2003, and the Ph.D. degree from the University of Surrey in 2009. In 2004, he joined the Centre for Biomedical Engineering, University of Surrey. He is currently an Assistant Professor with the Department of Electrical Engineering, Qatar University. His research interests include electronics, micro-engineering, neuroengineering, ac-electrokinetics, biomedical instrumentation, and biomedical signal processing. He is also currently serving as an Associate Editor of the IEEE TRANSACTIONS NANO BIOSCIENCE journal.